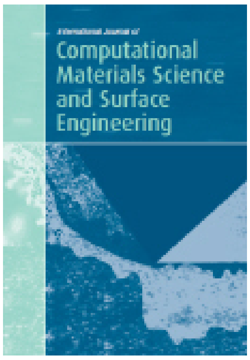

International Journal of Computational Materials Science and Surface Engineering

ISSN online: 1753-3473 - ISSN print: 1753-3465
https://www.inderscience.com/ijcmsse

Predicting the tensile behaviour of friction stir welded AA2024 and AA5083 alloy based on artificial neural network and mayfly optimisation algorithm

P.M. Diaz, M. Julie Emerald Jiju

DOI: 10.1504/IJCMSSE.2023.10053477

Article History:

Received:	30 September 2021
Accepted:	14 August 2022
Published online:	08 January 2024

Predicting the tensile behaviour of friction stir welded AA2024 and AA5083 alloy based on artificial neural network and mayfly optimisation algorithm

P.M. Diaz*

Dedicated Juncture Researcher's Association,
Kulasekharam, Kanyakumari, 629161, Tamil Nadu, India
Email: pauldiaz71@gmail.com
*Corresponding author

M. Julie Emerald Jiju

Department of MCA,
CSI Institute of Technology, Thovalai,
Kanyakumari, 629302, Tamil Nadu, India
Email: jijudiaz45@gmail.com

Abstract: The necessity of aluminium based metal matrix composites are growing rapidly in various fields especially in automobiles. To predict the tensile behaviour of AA2024 and AA5083 alloys, a new approach has been proposed by integrating the artificial neural network with mayfly optimisation algorithm (MOA). To analyse the predicting efficiency of the proposed approach, it is compared with artificial neural networks and experimental test values. For predicting the ultimate tensile strength of AA2024 and AA5083 alloys, the proposed approach achieved very less absolute error and mean absolute error of 0.0147% and 0.3680% respectively. Similarly, the prediction of the tensile elongation of AA2024 and AA5083 alloys, the proposed ANN-MOA approach achieved very less absolute error and mean absolute error of 0.0017% and 0.3269% respectively. The results from the analysis indicated that the proposed approach has enhanced predicting accuracy than artificial neural networks.

Keywords: aluminium alloy; mechanical properties; ANN; artificial neural network; mayfly optimisation algorithm; inertial weights.

Reference to this paper should be made as follows: Diaz, P.M. and Jiju, M.J.E. (2023) 'Predicting the tensile behaviour of friction stir welded AA2024 and AA5083 alloy based on artificial neural network and mayfly optimisation algorithm', *Int. J. Computational Materials Science and Surface Engineering*, Vol. 11, Nos. 3/4, pp.163–186.

Biographical notes: P.M. Diaz received his BE degree in the Department of Mechanical Engineering from Manonmaniam Sundaranar University, India in 1997, ME degree in Thermal Engineering from Bharathiar University in 2002, and PhD in Internal Combustion Engine from Sathyabama University in 2012. He is currently working as Associate Professor in the Department of Mechanical Engineering, Ponjesly College of Engineering, India. His research interests are IC engines, bio-fuel, machine learning, and deep learning.

M. Julie Emerald Jiju received her Bachelor of Computer Science degree in 1999 from Manonmaniam Sundaranar University, Master of Computer Applications degree in 2002 from Manonmaniam Sundaranar University, Master of Technology degree in 2004 from Manonmaniam Sundaranar University and Master of Philisophy in 2008 from Manonmaniam Sundaranar University. She is working as an Assistant Professor in the Department of MCA at C.S.I Institute of Technology. Her areas of interest are cloud computing and artificial intelligence.

1 Introduction

Nowadays, several engineering application in the world require materials having typical combination of properties which are better than the conventional metal alloys, polymers or ceramics. The components in the composite materials can be known macroscopically while in conventional metal alloy the components can be only identified by microscopic examination or higher magnification (Sarada et al., 2015). Metal matrix composites (MMCs) have many improved properties and hence they are used in several applications. These MMC materials are studied and formulated by combining the necessary characteristics of different metals (Mazahery and Shabani, 2012). MMCs can be used as the efficient alternative to the conventional alloy especially in stiffness and high strength applications (Shorowordi et al., 2003). Aluminium alloy is a type of matrix composite that has excellent mechanical properties such as light weight, high corrosion resistance, and high strength-to-weight ratio (Sevik and Kurnaz, 2006). Cost is the major drawback of MMCs for wider application in industries, but it can be compensated by its advantages in weight saving, improved recyclability, increased component life (Klimowicz, 1994; Hashim et al., 2001).

Metal matrix has certain benefits like preserving the strength at high temperature, low thermal shock, decreased part weight, wear resistance and higher specific strength when compared with conventional materials (Muthukrishnan et al., 2012). Also, mechanical and physical properties of MMCs can be customised for meeting specific design criteria. Hence, it is appropriate for variety of applications (Gurusamy et al., 2015). Aluminium and its alloys are broadly utilised as cylinder liner, brake rotor, drive shafts and pistons in automobile industry (Naher et al., 2003). The type of fabrication technique utilised in the manufacturing process greatly influence the properties of aluminium matrix composites (AMCs). Generally, both liquid and solid state fabrication techniques are utilised in alloy composite manufacturing process (Hajjari et al., 2011). Aluminium alloy plays an important role in engineering and automotive industries because of its wear resistance properties (Rahman et al., 2019). The aluminium alloys AA5083 and AA2024 are widely utilised in fabricating the aircraft structures and other structural components. Hence, these two alloys undergo dissimilar welding and are extensively applied during the fabrication process.

The friction stir welding (FSW) method is suitable for dissimilar welding process of AA2024 and AA5083aluminium alloys, because fusion welding procedures are not suited for dissimilar welding. The FSW is the process of joining the aluminium alloys that are hard to weld by conventional fusion methods which includes aluminium alloys with limited weldability (Flores et al., 1998; Murr et al., 1998). This method is suitable for producing the welded joints without bulk melting. The main advantage of FSW is that it is resistant to property deteriorations and defects related to fusion welding like coarsening and melting of strengthening phases. Hence, the weld produced by FSW shows enhanced mechanical properties like hardness, ductility and strength than the fusion welded alloys (Berbon et al., 2001; Lee et al., 2003; Sato et al., 2003). Artificial neural network is a developing technique to predict the response by training the network with experimental data (Zurada, 1992; Gurney, 1997). This technique is based on artificial intelligence which imitates the structure, mechanism and function of human brain (Elsheikh et al., 2019). These models can be effectively utilised for studying the materials with constitutive relations and it is also used to identify very complex non-linear phenomena (Singh et al., 2016; Dixit et al., 2017). Non-linear mathematical problems can be modelled using artificial neural network (ANN) since it has excellent generalisation capability (Elsheikh et al., 2020).

Recently, several meta-heuristic optimisation algorithms like particle swarm optimisation (PSO), whale optimisation algorithm, Harris hawks optimisation, artificial bee colony, cat swarm optimisation and genetic algorithm are combined with ANN for determining the parameters and optimal ANN structure (Oliva et al., 2019). Zervoudakis and Tsafarakis (2020) recently proposed a metaheuristic optimisation algorithm called mayfly optimisation algorithm (MOA) which imitates the social behaviour of mayflies. In this study, a new approach for predicting the mechanical properties of aluminium MMCs is presented. The hybridised metal utilised here is A413 aluminium alloy reinforced with 5% silicon carbide and 5% flyash. The proposed approach is modelled by integrating ANN with recently proposed metaheuristic algorithm known as MOA. Also, to improve the performance of MOA, different inertial weights are employed. This proposed model is utilised for predicting the mechanical properties of aluminium alloy.

2 Methodology

2.1 Artificial neural network

Artificial neural networks (ANNs) are widely used machine learning algorithms that are applied in several approaches due to their high classification performance. ANNs consists of neurons which are capable of extracting information from the dataset even in noisy data (Ledesma et al., 2008). They are universal function approximation algorithms for modelling both linear and non-linear data with required accuracy. Using different interconnection approaches, various kinds of neural networks are modelled in the data mining field. ANNs have many advantages such as easily adapting to different kinds of data, arbitrary decision boundary capabilities and their non-parametric nature. Typically, the learning of training data in neural networks takes place in an iterative way in which it considers all the patterns in the dataset for learning. Therefore, ANNs are called as the data dependent models (Kavzoglu and Mather, 2000). In ANN, the network weights are adjusted during training process until the actual output of the network and desired output of the network are as close as possible. Hence, ANNs can be effectively utilised for mapping an input to a desired output, for classifying data and for learning the patterns in the dataset provided. The commonly utilised neural network model is the feed forward neural network which is a multilayer perceptron. Figure 1 shows the structure of ANN model.

Figure 1 Structure of artificial neural network (see online version for colours)

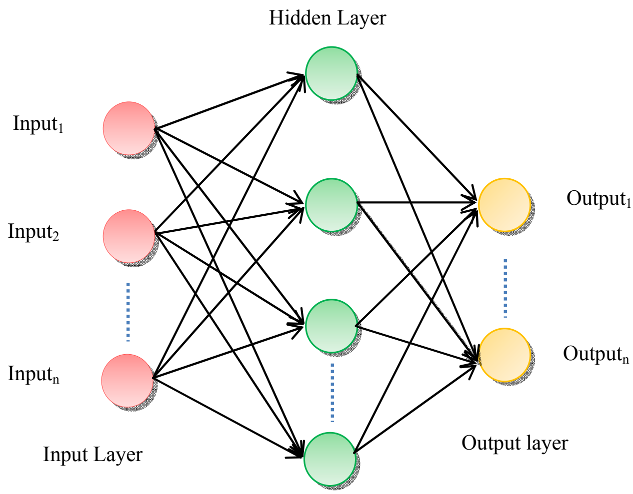

The FFNN consist of three types of units such as input unit, hidden unit and output unit. The initial unit is the known as the input unit and it is utilised for mapping the variables in the network. The final unit is the output unit and the units between input and output unit is known as hidden units. These units have processing nodes which are fully connected with one another and they do not have any interconnections among the nodes within the same layer. Here, the network is represented by directed graphs, the units are represented by nodes and the connections among them are represented by arcs. Each arc has a value which is the connection weight among a pair of units (Mavrovouniotis and Yang, 2015). In the neural network model, all connections from input unit is directed towards the hidden unit and then to the output unit. Here, the interconnection of neurons will be in one-directional and one-way approach. The connections are denoted as weights that are real numbers in the range [–1, 1].

In each node of the network, the output is computed in two phases. Initially, the summation weight of the input is computed as illustrated in equation (1).

$$S_j = \sum_{i=1}^{n} w_{ij} I_i + \beta_j \tag{1}$$

where w_{ij} denotes the connection weights between I_i and j, while I_i denotes the ith input variable, j denotes the hidden neuron, n is represented as the total number of neurons and β_j is denoted as the bias weight of jth hidden neuron.

Then, based on the weighted summation, the output of each node in hidden unit is determined. Here, the activation function is utilised for triggering the output depending on the summation function value. In neural networks, different kinds of activation function can be employed based on its requirement. In this approach, the hidden layer outputs are calculated using the sigmoid activation function which is illustrated in equation (2).

$$f_j(x) = \frac{1}{1 + e^{-S_j}} \tag{2}$$

Next the output of each neuron in the hidden unit will be calculated. Equation (3) illustrates the final output of ANN.

$$\hat{y}_k = \sum_{i=1}^{m} W_{kj} f_i + \beta_k \tag{3}$$

2.2 *Mayfly optimisation algorithm*

Mayfly optimisation algorithm is the metaheuristic algorithm which is stimulated from the behaviour of mayflies. Generally, the mayflies live in water at larvae stage for many years and then they grow into insects with wings. The life span of these mayflies will be from one day to seven days. During their life time, they will be busy in finding their partners for mating and reproduction. This behaviour of mayflies gives inspiration for the MOA.

In MOA, the female mayfly will be represented as $y_i(t)$ and the male mayfly will be represented as $x_i(t)$ for *i*th individual in current iteration *t*. The position of these mayflies will be updated with velocity $v_i(t)$ in current iteration as illustrated in equation (4).

$$p_i(t+1) = p_i(t) + v_i(t) \tag{4}$$

The velocity update for female and male mayflies will be in different ways. Equation (5) gives the velocity update for female mayflies.

$$v_i(t) = \begin{cases} g \cdot v_i(t) + a_1 e^{-\beta r_{mf}^2} \left[x_i(t) - y_i(t) \right] f[y_i(t)] > f[x_i(t)] \\ g \cdot v_i(t) + fl.r_1 \; [y_i(t)] \le f[x_i(t)] \end{cases} \tag{5}$$

where $f(x)$ is denoted as the fitness function, r_1 denotes the random number in uniform distribution ranging from –1 to 1, g and fl are weights that can be declined from its maximum to minimum value, a_1 is an attractive constant and β represents the visibility coefficient, and r_{mf} is denoted as the Cartesian distance between the male and female mayfly which is computed as given in equation (6).

$$\left\| x_i - y_j \right\| = \sqrt{\sum_{k=1}^{n} (x_{ik} - y_{ik})^2} \tag{6}$$

The velocity update for the male mayflies is given in equation (7).

$$v_i(t) = \begin{cases} g \cdot v_i(t) + a_2 e^{-\beta r_p^2} \left[x_{h_i} - x_i(t) \right] + a_3 e^{-\beta r_g^2} \left[x_g - x_i(t) \right] f[x_i(t)] > f[x_{hi}(t)] \\ g \cdot v_i(t) + d \cdot r_2 f[x_i(t)] \le f[x_{hi}(t)] \end{cases} \tag{7}$$

where, r_2 represents another random number ranging from –1 to 1, d is denoted as the dance ratio near the current position, x_{hi} is denoted as the ith historical best trajectory, x_g denotes the global best candidate, r_p and r_g are denoted as the Cartesian distance between $x_i(t)$, x_{h_i} and x_g, a_2 and a_3 are denoted as the position attraction constants used to measure the contribution of social and cognitive components.

After completing the velocity update, the mayflies will again reselect themselves. In the group, half of the mayflies will be selected as the male mayflies and the other half mayflies in the group will be considered as the female mayflies. Here, the best male mayfly mates with the best female mayfly and the offsprings are produced after a crossover as illustrated in equations (8) and (9).

$$offspring1 = L * male + (1 - L) * female \tag{8}$$

$$offspring2 = L * female + (1 - L) * male \tag{9}$$

Then, the offspring will undergo mutation process for enhancing the exploration ability of the algorithm. And after completing the current iteration, the offspring will grow up and based on their fitness values and they will be sorted. After that, they will be again nominated as female or male for the succeeding iterations.

2.3 MOA with varying inertial weights

MOA is a hybrid method which is developed by combining the benefits of other optimisation algorithms like PSO (Kennedy and Eberhart, 1995), genetic algorithm (GA) (Goldberg and Kennedy, 1988) and firefly algorithm (FA) (Yang and He, 2013). Generally, PSO has many advantages like easy implementation, faster convergence and fewer parameters. But it gets trapped in the local optimum. Since MOA has the characteristics of PSO algorithm, the necessary modifications are performed on MOA to have better performance. Thus, to overcome the drawback of getting trapped in the local optimum, inertial weights are introduced which effectively increase the diversity of the particles and gives better control over exploration and exploitation.

The inertial weight (ω) determines the local and global searching potential of the algorithm which is necessary for the particle to find the optimum solution. Hence, it strongly influences the overall performance of the algorithm. If the inertial weight is set as constant, the results will not be satisfactory because of its failure in balancing the global and local search. Thus, many inertial weighting methods have been developed for solving this problem. Initially, Nickabadi et al. (2011) developed a linear decreasing weight method which is illustrated in equation (10).

$$\omega_1(t) = \frac{t_{max} - t}{t_{max}}(\omega_{max} - \omega_{min}) + \omega_{min} \tag{10}$$

Also, it is known that the relatively smaller value of inertial weight will increase the local search ability and the larger value of inertial weight will increase the global search. For solving this problem, an inertial weighting technique has been proposed by Eberhart et al. (Eberhart and Shi, 2000) as given in equation (11) where the inertial weight is linearly decreased from 0.9 to 0.4.

$$\omega_2(t) = \begin{cases} 1 \times \dfrac{t}{t_{max}} + 0.4, \left(0 \le \dfrac{t}{t_{max}} \le 0.5\right) \\ -1 \times \dfrac{t}{t_{max}} + 1.4, \left(0.5 \le \dfrac{t}{t_{max}} \le 1\right) \end{cases} \tag{11}$$

Then, a non-linear decreasing strategy was developed by Chen et al. (Guimin et al., 2006) for updating the inertial weight as illustrated in equation (12). They stated that, in most of the continuous optimisation problems, the concave function performance depending on decreasing inertial weight is superior to the linear function.

$$\omega_3(t) = -(\omega_{start} - \omega_{end})\left(\frac{t}{t_{max}}\right)^2 + \omega_{start} \tag{12}$$

Finally, the sigmoid-like inertial weight (Tian and Shi, 2018) is proposed for combining the inertial weight and non-linear weight which balances both the local and global search ability. It is based on sigmoid and it is illustrated as given in equation (13).

$$\omega_4(t) = \begin{cases} 0.9, & (t \le \alpha t_{max}, \alpha = 0.2) \\ \dfrac{1}{1 + e^{(10t - 2t_{max})/t_{max}}} + 0.4, & (otherwise) \end{cases} \tag{13}$$

In deep learning, the sigmoid is the widely utilised activation function and it can accurately attain the trade-off between linear and non-linear function. Here, ω_{min} and ω_{max} are denoted as the final value and initial value of inertial weight. While, t_{max} and t are denoted as the maximum number of iterations and current iteration.

2.4 Proposed approach

In the proposed method, MOA with varying inertial weights is utilised for training the artificial neural network. The convergence and performance of training process in ANN is influenced by the initialisation of connection weights and biases. Hence, in the proposed approach, MOA is utilised on the search space for finding the optimal value of initial weights and biases. This process of initialising the weights and biases using optimal values will result in better convergence and prediction accuracy. Here, MOA is utilised to train the ANN with single hidden unit. While modelling the proposed approach, the selection of fitness function and the representation of search agents should be taken in consideration. In this process, each search agent will be predetermined as one dimensional vector for representing the optimistic neural network. The proposed model consist of three parts such as connection weights linking input unit and hidden unit, connection weights linking hidden unit and output unit and biases. The flow of the proposed model is given in Figure 2.

Figure 2 Flowchart of the proposed MOA-ANN model (see online version for colours)

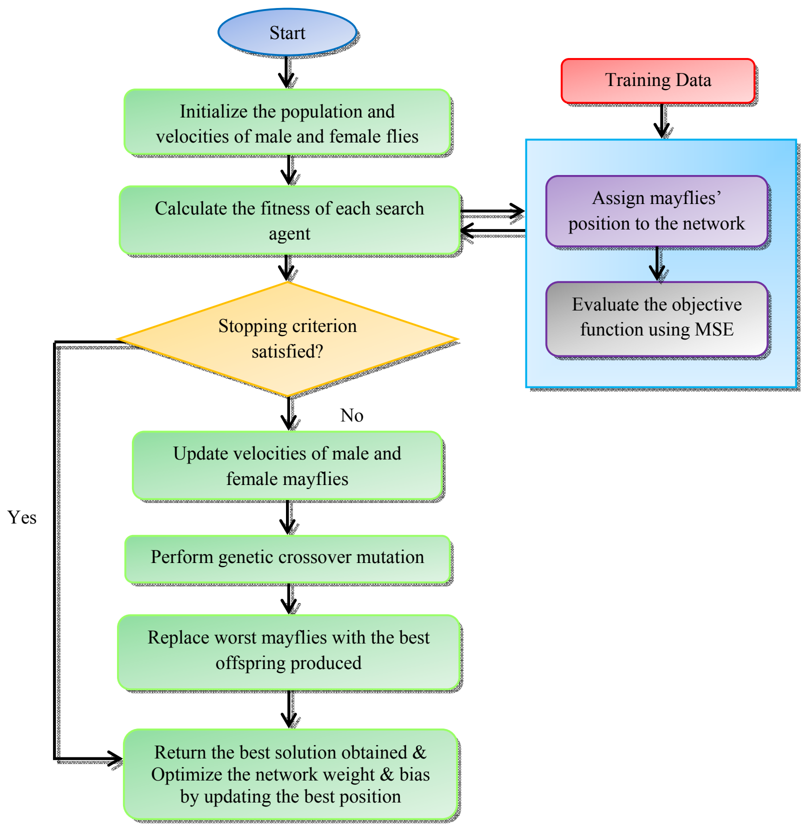

Here, each solution is taken as the vector of real number with an interval of –1 to 1. Also, each vector length equalises the total number of biases and weights in the network which is calculated as given in equation (14).

$$vector\,length = (n \times m) + (2 \times m) + 1 \tag{14}$$

where m denotes number of nodes present in hidden units and n denotes number of input features in the dataset.

Then, mean squared error (MSE) have been utilised for measuring the fitness function of the MOA. It is defined as the measure of difference between the actual values and the predicted values generated by neural networks for all training data. The MSE measure is illustrated in equation (15).

$$MSE = \frac{1}{n}\sum_{i=1}^{n}(y_i - \hat{y}_i)^2 \tag{15}$$

where n denotes the number of samples in training dataset, $\hat{y}_i$ denotes the predicted output and y_i is denoted as the actual output. After selecting the fitness function and defining the representation of solutions, the MOA will be utilised for training neural networks.

3 Materials and methods

Experimental data from the literature (Sundaram and Murugan, 2010) was used to evaluate the suggested model. The sample of these experimental data are shown in Tables 1 and 2. The FS Welded joints were made from the aluminium alloys AA5083 and AA2024. The different joints were created using the FSW setup. The joints were created with five distinct tools made of high-speed steel (HSS) with varied pin profiles: Paddle Shape (PS), Tapered Cylinder with Grooves (CG), Straight Cylinder (SC), Tapered Square (TS), and Tapered Hexagon (TH). The impact of toolpin profile (P), welding speed (S), axial plunge force (F), and rotational speed (N) on welded joint tensile behaviour has been investigated. Three tensile specimens were taken from FS Welded joints and prepared to ASTM E8M-04 specifications. The tensile elongation and UTS were measured.

Table 1 Sample experimental data of UTS used in the suggested model

Trial run	*FSW process parameters*				*TE(%)*		
	P	*N*	*S*	*F*	*Experimental*	*Predicted*	*Error%*
1	–1	–1	–1	–1	281.9	269.4	4.6
2	1	–1	–1	–1	260.3	256.5	1.5
3	–1	1	–1	–1	263.4	256.5	2.7
4	1	1	–1	–1	274.5	269.4	1.9
5	–1	–1	1	–1	282.7	269.4	4.9
6	1	–1	1	–1	261.2	256.5	1.8
7	–1	1	1	–1	264.3	256.5	3.0
8	1	1	1	–1	275.0	269.4	2.1
9	–1	–1	–1	1	272.2	269.4	1.0
10	1	–1	–1	1	249.4	256.5	–2.8

Table 2 Sample experimental data of TE used in the suggested model

Trial run	*FSW process parameters*				*TE*(%)		
	P	*N*	*S*	*F*	*Experimental*	*Predicted*	*Error%*
1	–1	–1	–1	–1	12.1	12.1	0.0
2	1	–1	–1	–1	11.6	11.7	–1.0
3	–1	1	–1	–1	9.6	9.3	3.3
4	1	1	–1	–1	9.4	8.9	5.4
5	–1	–1	1	–1	14.5	14.2	1.8
6	1	–1	1	–1	14.1	13.9	1.7
7	–1	1	1	–1	12.0	12.4	–2.9
8	1	1	1	–1	11.9	12.0	–0.7
9	–1	–1	–1	1	11.5	11.1	3.3
10	1	–1	–1	1	11.2	10.8	4.1

4 Results and discussions

In this study, ANN-MOA algorithm with varying inertial weights is proposed for prediction process. To demonstrate the accuracy of ANN-MOA algorithm, the results are compared with ANN and the actual experimental results. Before testing, the ANN-MOA model is trained with 70% of data and the remaining 30% of data is used for testing the performance of proposed model. The experimental process is conducted for parameters like tensile elongation and ultimate tensile strength. The ANN-MOA algorithm is experimented with varying weights ($\omega_1, \omega_2, \omega_3$ and ω_4) and the results are estimated. The proposed model has attained higher prediction results for all the parameters utilised in the comparison process and the ANN model has attained lesser predictability than the proposed model. Thus, the correlation between ANN-MOA predicted data and the corresponding experimental data is better than those obtained by ANN model. This shows that the integration between the ANN and metaheuristic technique (MOA) have successfully predicted the experimental values.

4.1 Validation of ANN-MOA model

In order to validate the proposed ANN-MOA model, the actual results are compared with the predicted results of ANN and ANN-MOA with four different inertial weights. The proposed method is utilised for predicting the tensile behaviour like UTS and TS for AA5083 and AA2024 aluminium alloys.

Figures 3–7 gives the comparison results for tensile elongation of AA2024 and AA5083 alloys. Here, the actual values are compared with predicted values of ANN and proposed model at varying inertial weights. In this process, the proposed model has predicted better values than ANN for all the four weights. Also, among the four inertial weights, ω_2 and ω_4 has attained higher success rate than the other inertial weights. Hence, the results show that the proposed method has better prediction accuracy for the tensile elongation of aluminium alloy.

Figure 3 Comparison of actual values with predicted values of ANN for tensile elongation (see online version for colours)

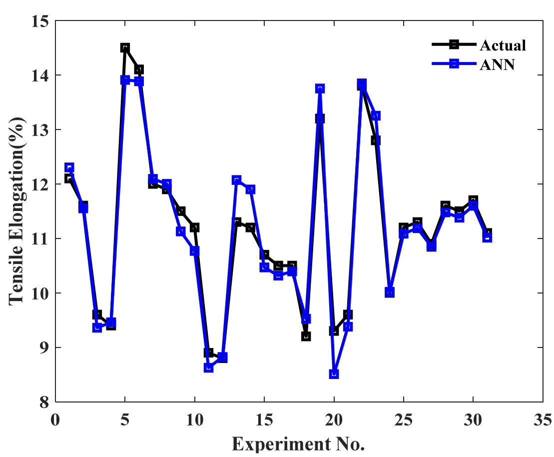

Figure 4 Comparison of actual values with predicted values of ANN-MOA(ω_1) for tensile elongation (see online version for colours)

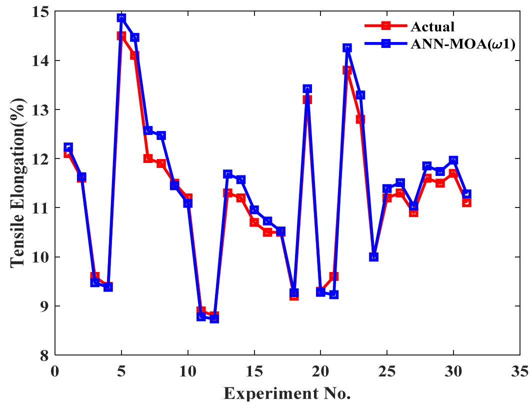

Figure 5 Comparison of actual values with predicted values of ANN-MOA(ω_2) for tensile elongation (see online version for colours)

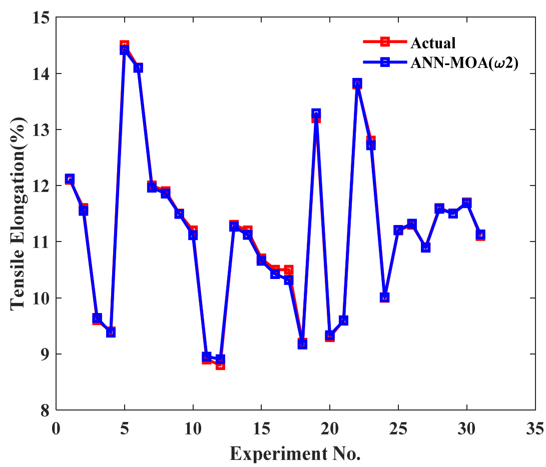

Figure 6 Comparison of actual values with predicted values of ANN-MOA (ω_3) for tensile elongation (see online version for colours)

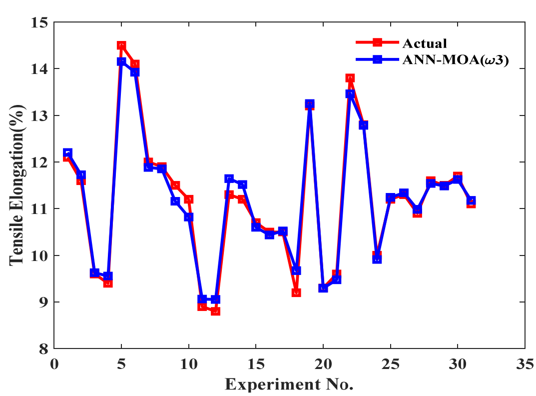

Figure 7 Comparison of actual values with predicted values of ANN-MOA (ω_4) for tensile elongation (see online version for colours)

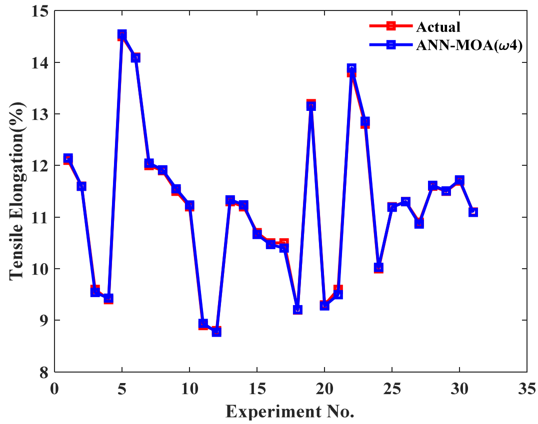

To analyse the effectiveness of the proposed method in terms of tensile elongation prediction, MSE for four different inertial weights at varying iterations varying weights of ANN-MOA is considered. Figure 8 illustrates that the inertial weight ω_3-MOA evolves faster and converges quickly towards the best solution than the other inertial weights. It is observed that the other inertial weights are comparatively slower than inertial weight ω_3-MOA. In this process, 30 independent runs are conducted with each run being 100 iterations.

Figure 8 MSE for varying weights of ANN-MOA in tensile elongation (see online version for colours)

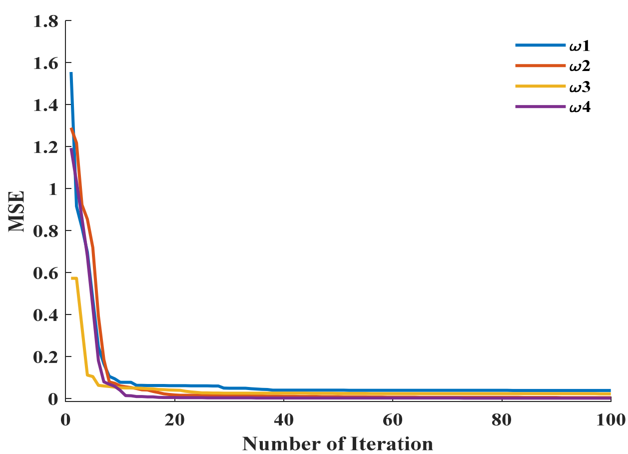

Figures 9–13 gives the comparison results for ultimate tensile strength of AA2024 and AA5083 alloys. Here, the actual values are compared with predicted values of ANN and proposed model at varying inertial weights. In this process, the proposed model has

predicted better values than ANN for all the four weights. Also, among the four inertial weights, ω_3 and ω_4 has attained higher success rate than the other inertial weights. Hence, the results show that the proposed method has better prediction accuracy for the ultimate tensile strength of aluminium alloy.

Figure 9 Comparison of actual values with predicted values of ANN for ultimate tensile strength (see online version for colours)

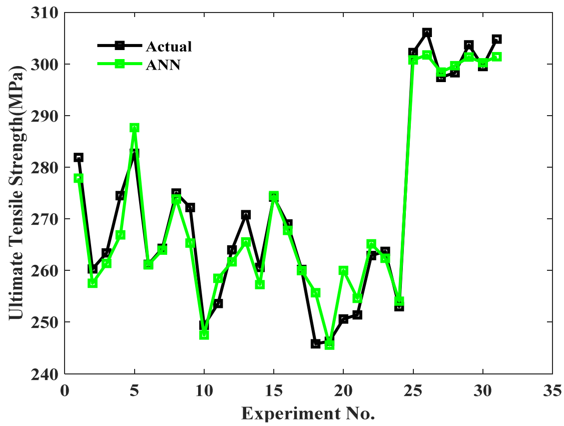

Figure 10 Comparison of actual values with predicted values of ANN-MOA(ω_1) for ultimate tensile strength (see online version for colours)

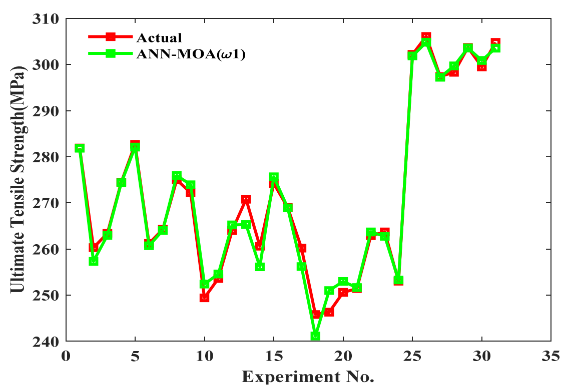

To analyse the effectiveness of the proposed method in terms of ultimate tensile strength prediction, MSE for four different inertial weights at varying iterations varying weights of ANN-MOA is considered. Figure 14 illustrates that the inertial weight ω_4-MOA evolves faster and converges quickly towards the best solution than the other inertial weights. It is observed that the other inertial weights are comparatively slower than inertial weight ω_4-MOA. In this process, 30 independent runs are conducted with each run being 100 iterations.

Figure 11 Comparison of actual values with predicted values of ANN-MOA(ω_2) for ultimate tensile strength (see online version for colours)

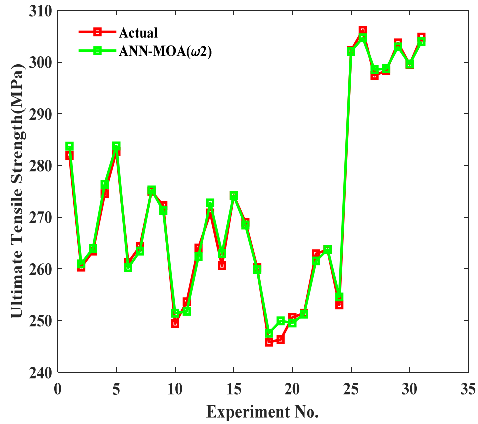

Figure 12 Comparison of actual values with predicted values of ANN-MOA (ω_3) for ultimate tensile strength (see online version for colours)

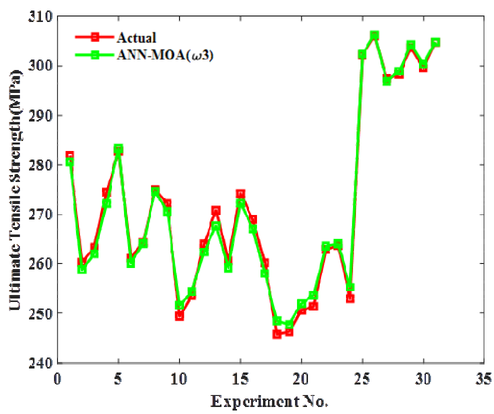

Figure 13 Comparison of actual values with predicted values of ANN-MOA(ω_4) for ultimate tensile strength (see online version for colours)

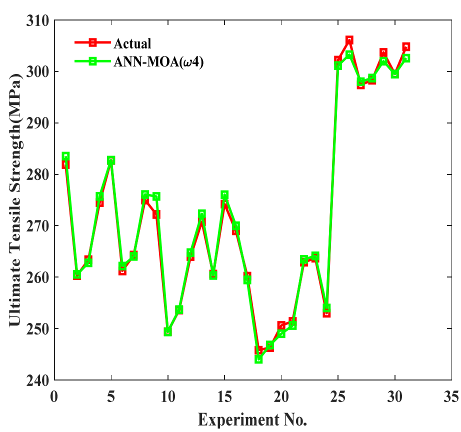

Figure 14 MSE for varying weights of ANN-MOA in ultimate tensile strength (see online version for colours)

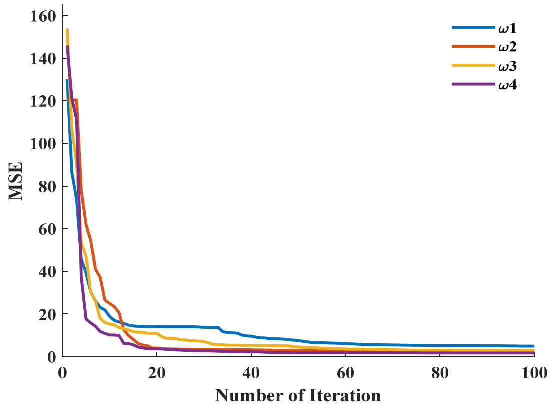

The data are trained and tested using the proposed ANN-MOA model and the percentage of error is computed using equation (14).

$$Percentage\, of\ error\ \% = \frac{Actual\ value - Predicted\ value}{Actual\ value} \times 100 \quad (14)$$

Table 3 gives the predicted error in ultimate tensile strength of AA2024 and AA5083 alloys using ANN-MOA model with varying inertial weights. The predicted error in proposed method is very less compared to the actual values. Hence, the results show that the proposed method has better prediction accuracy for the ultimate tensile strength of aluminium alloy.

Table 3 Predicted error in ultimate tensile strength of AA2024 and AA5083 alloys using ANN-MOA model with varying inertial weights

Predicted error				*Actual UTS*
w1	*w2*	*w3*	*w4*	
0.0660	–1.8336	1.2924	–1.6317	281.9
2.9864	–0.6463	1.4506	–0.2338	260.3
0.4335	–0.5462	1.3781	0.6160	263.4
0.1261	–1.8274	2.3235	–1.2083	274.5
0.6066	–1.0553	–0.5676	–0.0361	282.7
0.5023	0.9940	1.0991	–0.9528	261.2
0.2705	0.8864	0.2238	0.2813	264.3
–0.9377	–0.2377	0.3878	–1.0726	275
–1.7412	0.9358	1.6393	–3.4898	272.2
–2.9954	–2.0060	–2.2386	0.0472	249.4
–0.9794	1.8420	–0.7714	–0.1046	253.6
–1.2214	1.6301	1.6186	–0.7569	264
5.4994	–1.9490	3.1394	–1.5106	270.8

Table 3 Predicted error in ultimate tensile strength of AA2024 and AA5083 alloys using ANN-MOA model with varying inertial weights (continued)

Predicted error				*Actual UTS*
w1	*w2*	*w3*	*w4*	
4.4684	–2.3332	1.3781	0.2716	260.6
–1.4508	0.0475	1.9607	–1.8363	274.2
0.0865	0.5460	1.9193	–0.9780	269
4.0150	0.3679	2.1642	0.7293	260.2
4.6706	–1.7249	–2.6979	1.7812	245.8
–4.7027	–3.6265	–1.4514	–0.5074	246.3
–2.3661	1.0970	–1.4308	1.6052	250.6
–0.2292	0.1933	–2.2440	0.7938	251.4
–0.7888	1.3903	–0.6923	–0.5644	262.9
0.9570	–0.0316	–0.3554	–0.4330	263.7
–0.2747	–1.5476	–2.2743	–1.0064	253
0.3366	0.1556	–0.1942	1.0765	302.2
1.2645	1.4033	–0.2605	2.8347	306.1
0.1732	–1.1261	0.4801	–0.6077	297.4
–1.3991	–0.4079	–0.6503	–0.3959	298.3
0.1176	0.7682	–0.6001	1.7136	303.7
–1.3798	–0.1074	–0.8453	0.0259	299.5
1.2501	0.8556	–0.0448	2.2239	304.8

Table 4 gives the absolute error and mean absolute error for aluminium alloy in ANN-MOA model with varying inertial weights in terms of ultimate tensile strength. The proposed method has lesser absolute error (0.0147 %) and mean absolute error (0.3680 %) for all inertial weights. Hence, the results show that the proposed method has better prediction accuracy for the tensile behaviour of aluminium alloy.

Table 4 Absolute error and mean absolute error for ultimate tensile strength of AA2024 and AA5083 alloys using ANN-MOA model with varying weights

Absolute error %			
AE1	*AE2*	*AE3*	*AE4*
0.0234	0.6504	0.4585	0.5788
1.1473	0.2483	0.5573	0.0898
0.1646	0.2074	0.5232	0.2339
0.0459	0.6657	0.8465	0.4402
0.2146	0.3733	0.2008	0.0128

Table 4 Absolute error and mean absolute error for ultimate tensile strength of AA2024 and AA5083 alloys using ANN-MOA model with varying weights (continued)

Absolute error %			
AE1	*AE2*	*AE3*	*AE4*
0.1923	0.3806	0.4208	0.3648
0.1024	0.3354	0.0847	0.1064
0.3410	0.0864	0.1410	0.3900
0.6397	0.3438	0.6022	1.2821
1.2011	0.8043	0.8976	0.0189
0.3862	0.7263	0.3042	0.0413
0.4627	0.6175	0.6131	0.2867
2.0308	0.7197	1.1593	0.5578
1.7147	0.8953	0.5288	0.1042
0.5291	0.0173	0.7151	0.6697
0.0321	0.2030	0.7135	0.3636
1.5430	0.1414	0.8317	0.2803
1.9001	0.7017	1.0976	0.7247
1.9093	1.4724	0.5893	0.2060
0.9442	0.4378	0.5710	0.6406
0.0912	0.0769	0.8926	0.3157
0.3000	0.5288	0.2633	0.2147
0.3629	0.0120	0.1348	0.1642
0.1086	0.6117	0.8990	0.3978
0.1114	0.0515	0.0643	0.3562
0.4131	0.4584	0.0851	0.9261
0.0582	0.3787	0.1614	0.2043
0.4690	0.1367	0.2180	0.1327
0.0387	0.2529	0.1976	0.5643
0.4607	0.0359	0.2822	0.0086
0.4101	0.2807	0.0147	0.7296
MAE %			
0.5919	0.4146	0.4861	0.3680

Table 5 gives the predicted error in ultimate tensile strength of AA2024 and AA5083 alloys using ANN-MOA model with varying inertial weights. The predicted error in proposed method is very less compared to the actual values. Hence, the results show that the proposed method has better prediction accuracy for the tensile behaviour of aluminium alloy.

Table 5 Predicted error in tensile elongation of AA2024 and AA5083 alloys using ANN-MOA model with varying inertial weights

Predicted error				
w1	*w2*	*w3*	*w4*	*Actual TE*
–0.1349	–0.0251	–0.1038	–0.0464	12.1
–0.0314	0.0523	–0.1260	0.0042	11.6
0.1270	–0.0400	–0.0269	0.0591	9.6
0.0209	0.0212	–0.1571	–0.0305	9.4
–0.3653	0.0865	0.3487	0.0488	14.5
–0.3674	0.0036	0.1771	0.0152	14.1
–0.5718	0.0388	0.1168	–0.0460	12
–0.5699	0.0429	0.0470	–0.0170	11.9
0.0520	0.0062	0.3415	–0.0497	11.5
0.1127	0.0843	0.3780	–0.0361	11.2
0.1195	–0.0515	–0.1635	–0.0414	8.9
0.0642	–0.1060	–0.2550	–0.0308	8.8
–0.3843	0.0333	–0.3445	–0.0358	11.3
–0.3712	0.0801	–0.3180	–0.0382	11.2
–0.2570	0.0425	0.0974	0.0369	10.7
–0.2295	0.0778	0.0630	0.0315	10.5
–0.0265	0.1822	–0.0231	0.1000	10.5
–0.0697	0.0335	–0.4726	–0.0067	9.2
–0.2224	–0.0865	–0.0527	0.0511	13.2
0.0228	–0.0332	0.0047	0.0210	9.3
0.3709	0.0081	0.1223	0.1023	9.6
–0.4555	–0.0271	0.3401	–0.0891	13.8
–0.4952	0.0832	0.0141	–0.0591	12.8
0.0058	–0.0078	0.0895	–0.0268	10
–0.1905	–0.0086	–0.0427	0.0085	11.2
–0.2106	–0.0211	–0.0398	0.0002	11.3
–0.1353	0.0086	–0.0860	0.0347	10.9
–0.2505	0.0149	0.0598	–0.0154	11.6
–0.2361	0.0002	0.0136	–0.0071	11.5
–0.2668	0.0139	0.0754	–0.0204	11.7
–0.1822	–0.0294	–0.0763	0.0095	11.1

Table 6 gives the absolute error and mean absolute error for AA2024 and AA5083 aluminium alloy in ANN-MOA model with varying inertial weights in terms of tensile elongation. The proposed method has lesser absolute error (0.0017%) and mean absolute error (0.3269 %) for all inertial weights. Hence, the results show that the proposed method has better prediction accuracy for the tensile behaviour of aluminium alloy.

Table 6 Absolute error and mean absolute error for tensile elongation of AA2024 and AA5083 alloys using ANN-MOA model with varying weights

Absolute Error %			
AE1	*AE2*	*AE3*	*AE4*
1.1153	0.2077	0.8582	0.3839
0.2705	0.4513	1.0864	0.0364
1.3232	0.4170	0.2801	0.6153
0.2223	0.2258	1.6714	0.3248
2.5194	0.5968	2.4046	0.3368
2.6059	0.0257	1.2559	0.1076
4.7652	0.3235	0.9735	0.3836
4.7894	0.3602	0.3950	0.1431
0.4522	0.0539	2.9696	0.4318
1.0065	0.7523	3.3751	0.3223
1.3428	0.5786	1.8366	0.4656
0.7299	1.2047	2.8979	0.3499
3.4009	0.2944	3.0489	0.3168
3.3139	0.7153	2.8394	0.3415
2.4023	0.3968	0.9104	0.3445
2.1858	0.7408	0.5999	0.2997
0.2524	1.7356	0.2199	0.9521
0.7571	0.3638	5.1371	0.0731
1.6845	0.6552	0.3995	0.3870
0.2454	0.3569	0.0502	0.2255
3.8636	0.0840	1.2741	1.0656
3.3008	0.1966	2.4642	0.6455
3.8684	0.6501	0.1098	0.4618
0.0577	0.0784	0.8955	0.2679
1.7008	0.0767	0.3808	0.0763
1.8633	0.1866	0.3520	0.0017
1.2415	0.0786	0.7891	0.3187
2.1594	0.1288	0.5159	0.1329
2.0526	0.0017	0.1183	0.0621
2.2807	0.1186	0.6444	0.1746
1.6413	0.2645	0.6875	0.0859
MAE %			
1.9166	0.3975	1.3368	0.3269

Table 7 gives the actual values by experimental process and predicted values by ANN-MOA model with varying inertial weights for ultimate tensile strength of AA2024 and AA5083 alloys. The proposed method has predicted nearly equal values relating to the actual values. Hence, the results show that the proposed method has better prediction accuracy for the tensile behaviour of aluminium alloy.

Table 7 Predicted values for ultimate tensile strength inAA2024 and AA5083 alloy using ANN-MOA model with varying weights

UTS				
	predicted			
Actual	*w1*	*w2*	*w3*	*w4*
281.9	281.8340	283.7336	280.6076	283.5317
260.3	257.3136	260.9463	258.8494	260.5338
263.4	262.9665	263.9462	262.0219	262.7840
274.5	274.3739	276.3274	272.1765	275.7083
282.7	282.0934	283.7553	283.2676	282.7361
261.2	260.6977	260.2060	260.1009	262.1528
264.3	264.0295	263.4136	264.0762	264.0187
275	275.9377	275.2377	274.6122	276.0726
272.2	273.9412	271.2642	270.5607	275.6898
249.4	252.3954	251.4060	251.6386	249.3528
253.6	254.5794	251.7580	254.3714	253.7046
264	265.2214	262.3699	262.3814	264.7569
270.8	265.3006	272.7490	267.6606	272.3106
260.6	256.1316	262.9332	259.2219	260.3284
274.2	275.6508	274.1525	272.2393	276.0363
269	268.9135	268.4540	267.0807	269.9780
260.2	256.1850	259.8321	258.0358	259.4707
245.8	241.1294	247.5249	248.4979	244.0188
246.3	251.0027	249.9265	247.7514	246.8074
250.6	252.9661	249.5030	252.0308	248.9948
251.4	251.6292	251.2067	253.6440	250.6062
262.9	263.6888	261.5097	263.5923	263.4644
263.7	262.7430	263.7316	264.0554	264.1330
253	253.2747	254.5476	255.2743	254.0064
302.2	301.8634	302.0444	302.3942	301.1235
306.1	304.8355	304.6967	306.3605	303.2653
297.4	297.2268	298.5261	296.9199	298.0077
298.3	299.6991	298.7079	298.9503	298.6959
303.7	303.5824	302.9318	304.3001	301.9864
299.5	300.8798	299.6074	300.3453	299.4741
304.8	303.5499	303.9444	304.8448	302.5761

Table 8 gives the actual values by experimental process and predicted values by ANN-MOA model with varying inertial weights for tensile elongation AA2024 and AA5083 alloys. The proposed method has predicted nearly equal values relating to the actual values. Hence, the results show that the proposed method has better prediction accuracy for the tensile behaviour of aluminium alloy.

Table 8 Predicted values in ANN-MOA model for tensile elongation

TE				
Actual	*Predicted*			
	w1	*w2*	*w3*	*w4*
12.1	12.2349459	12.1251	12.20383621	12.1464
11.6	11.63137508	11.5477	11.72602036	11.5958
9.6	9.472971553	9.6400	9.626891314	9.5409
9.4	9.379105503	9.3788	9.557107201	9.4305
14.5	14.8653155	14.4135	14.15133445	14.5488
14.1	14.46743135	14.0964	13.92291614	14.0848
12	12.57181873	11.9612	11.88317986	12.046
11.9	12.46993601	11.8571	11.85299896	11.917
11.5	11.44799152	11.4938	11.15849603	11.5497
11.2	11.0872742	11.1157	10.8219861	11.2361
8.9	8.780492299	8.9515	9.063459749	8.9414
8.8	8.735765448	8.9060	9.055013676	8.7692
11.3	11.68429951	11.2667	11.64453016	11.3358
11.2	11.57115129	11.1199	11.51801519	11.2382
10.7	10.95704716	10.6575	10.60259122	10.6631
10.5	10.72950982	10.4222	10.43701167	10.4685
10.5	10.52650447	10.3178	10.52309446	10.4
9.2	9.269652818	9.1665	9.672615017	9.2067
13.2	13.42235249	13.2865	13.25273005	13.1489
9.3	9.277174576	9.3332	9.295336035	9.279
9.6	9.229094883	9.5919	9.477688725	9.4977
13.8	14.25551296	13.8271	13.45994073	13.8891
12.8	13.29515777	12.7168	12.78594567	12.8591
10	9.99422751	10.0078	9.910454346	10.0268
11.2	11.39048417	11.2086	11.242653	11.1915
11.3	11.51055388	11.3211	11.33977387	11.2998
10.9	11.03531883	10.8914	10.98601123	10.8653
11.6	11.8504884	11.5851	11.54015616	11.6154
11.5	11.73605348	11.4998	11.48639401	11.5071
11.7	11.96684217	11.6861	11.62460306	11.7204
11.1	11.28218899	11.1294	11.17631522	11.0905

5 Conclusion

In this experimental process, the artificial neural networks with MOA are employed for predicting the tensile behaviour like tensile elongation and ultimate tensile strength for AA2024 and AA5083 alloys. The experimental results are conducted for one unforged specimen and three forged specimens at different directions. The predicted results from the proposed model are compared with actual results and ANN. From the results attained, it can be concluded that when the artificial neural networks are optimised by MOA, the prediction results are in admissible agreement with the experimental results. The proposed ANN-MOA approach achieved very less absolute error and mean absolute error of 0.0147% and 0.3680% respectively for the prediction of ultimate tensile strength of AA2024 and AA5083 alloys. Similarly, the proposed ANN-MOA approach achieved very less absolute error and mean absolute error of 0.0017% and 0.3269% respectively for the prediction of the tensile elongation of AA2024 and AA5083 alloys. Therefore, using ANN-MOA model instead of experiments will decrease the cost and need for special testing facilities and the ANN-MOA model can be used for optimising and predicting the effective parameters of MMCs. In future, other mechanical properties of aluminium alloys can be considered in the prediction process.

References

Berbon, P.B., Bingel, W.H., Mishra, R.S., Bampton, C.C. and Mahoney, M.W. (2001) 'Friction stir processing: a tool to homogenize nanocomposite aluminum alloys', *Scripta Materialia*, Vol. 44, No. 1, pp.61–66.

Dixit, M.C., Srivastava, N. and Rajput, S.K. (2017) 'Modeling of flow stress of AA6061 under hot compression using artificial neural network', *Materials Today: Proceedings*, Vol. 4, No. 2, pp.1964–1971.

Eberhart, R.C. and Shi, Y. (2000) 'Comparing inertia weights and constriction factors in particle swarm optimization', *Proceedings of the 2000 Congress on Evolutionary Computation. CEC00 (Cat. No. 00TH8512)*, IEEE, Vol. 1, July, pp.84–88.

Elsheikh, A.H., Sharshir, S.W., AbdElaziz, M., Kabeel, A.E., Guilan, W. and Haiou, Z. (2019) 'Modeling of solar energy systems using artificial neural network: a comprehensive review', *Solar Energy*, Vol. 180, pp.622–639.

Elsheikh, A.H., Sharshir, S.W., Ismail, A.S., Sathyamurthy, R., Abdelhamid, T., Edreis, E.M. and Haiou, Z. (2020) 'An artificial neural network based approach for prediction the thermal conductivity of nanofluids', *SN Applied Sciences*, Vol. 2, No. 2, pp.1–11.

Flores, O.V., Kennedy, C., Murr, L.E., Brown, D., Pappu, S., Nowak, B.M. and McClure, J.C. (1998) 'Microstructural issues in a friction-stir-welded aluminum alloy', *ScriptaMaterialia*, Vol. 38, No. 5, pp.703–708.

Goldberg, D.E. and Holland J.H. (1988) 'Genetic algorithms and machine learning', *Machine Learning*, Vol. 3, pp.95–99.

Guimin, C., Jianyuan, J. and Qi, H. (2006) 'Study on the strategy of decreasing inertia weight in particle swarm optimization algorithm', *Journal-Xian Jiaotong University*, Vol. 40, No. 1, p.53.

Gurney, K. (1997) *An Introduction to Neural Networks*, ISBN 0-203-45151-1 Master e-book, Imprint CRC Press, London.

Gurusamy, P., Prabu, S.B. and Paskaramoorthy, R. (2015) 'Influence of processing temperatures on mechanical properties and microstructure of squeeze cast aluminum alloy composites', *Materials and Manufacturing Processes*, Vol. 30, No. 3, pp.367–373.

Hajjari, E., Divandari, M. and Arabi, H. (2011) 'Effect of applied pressure and nickel coating on microstructural development in continuous carbon fiber-reinforced aluminum composites fabricated by squeeze casting', *Materials and Manufacturing Processes*, Vol. 26, No. 4, pp.599–603.

Hashim, J., Looney, L. and Hashmi, M.S.J. (2001) 'The enhancement of wettability of SiC particles in cast aluminium matrix composites', *Journal of Materials Processing Technology*, Vol. 119, Nos. 1–3, pp.329–335.

Kavzoglu, T. and Mather, P.M. (2000) 'The use of feature selection techniques in the context of artificial neural networks', *Proceedings of the 26th Annual Conference of the Remote Sensing Society*, September, Leicester, UK.

Kennedy, J. and Eberhart, R. (1995) 'Particle swarm optimization', *Proceedings of ICNN'95-International Conference on Neural Networks*, IEEE, Vol. 4, November, pp.1942–1948.

Klimowicz, T.F. (1994) 'The large-scale commercialization of aluminum-matrix composites', *JOM*, Vol. 46, No. 11, pp.49–53.

Ledesma, S., Cerda, G., Avina, G., Hernandez, D. and Torres, M. (2008) 'Feature selection using artificial neural networks', *Mexican International Conference on Artificial Intelligence*, October, Springer, Berlin, Heidelberg, pp.351–359.

Lee, W.B., Yeon, Y.M. and Jung, S.B. (2003) 'The improvement of mechanical properties of friction-stir-welded A356 Al alloy', *Materials Science and Engineering: A*, Vol. 355, Nos. 1–2, pp.154–159.

Mavrovouniotis, M. and Yang, S. (2015) 'Training neural networks with ant colony optimization algorithms for pattern classification', *Soft Computing*, Vol. 19, No. 6, pp.1511–1522.

Mazahery, A. and Shabani, M.O. (2012) 'Mechanical properties of squeeze-cast A356 composites reinforced with B_4C particulates', *Journal of Materials Engineering and Performance*, Vol. 21, No. 2, pp.247–252.

Murr, L.E., Liu, G. and McClure, J.C. (1998) 'A TEM study of precipitation and related microstructures in friction-stir-welded 6061 aluminium', *Journal of Materials Science*, Vol. 33, No. 5, pp.1243–1251.

Muthukrishnan, N., Babu, T.M. and Ramanujam, R. (2012) 'Fabrication and turning of Al/SiC/B4C hybrid metal matrix composites optimization using desirability analysis', *Journal of the Chinese Institute of Industrial Engineers*, Vol. 29, No. 8, pp.515–525.

Naher, S., Brabazon, D. and Looney, L. (2003) 'Simulation of the stir casting process', *Journal of Materials Processing Technology*, Vol. 143, pp.567–571.

Nickabadi, A., Ebadzadeh, M.M. and Safabakhsh, R. (2011) 'A novel particle swarm optimization algorithm with adaptive inertia weight', *Applied Soft Computing*, Vol. 11, No. 4, pp.3658–3670.

Oliva, D., AbdElaziz, M., Elsheikh, A.H. and Ewees, A.A. (2019) 'A review on meta-heuristics methods for estimating parameters of solar cells', *Journal of Power Sources*, Vol. 435, p.126683.

Rahman, A.A., Salleh, M.S., Othman, I.S., Subramonian, S., Yahaya, S.H. and Siswanto, N. (2019) 'Investigation of wear and corrosion characteristics of short heat treated thixoformed aluminium alloy', *Journal of Advanced Manufacturing Technology (JAMT)*, Vol. 13, No. 3, pp.97–108.

Sarada, B.N., Murthy, P.S. and Ugrasen, G. (2015) 'Hardness and wear characteristics of hybrid aluminium metal matrix composites produced by stir casting technique', *Materials Today: Proceedings*, Vol. 2, Nos. 4–5, pp.2878–2885.

Sato, Y.S., Urata, M., Kokawa, H. and Ikeda, K. (2003) 'Hall–Petch relationship in friction stir welds of equal channel angular-pressed aluminium alloys', *Materials Science and Engineering: A* Vol. 354, Nos. 1-2, pp.298–305.

Sevik, H. and Kurnaz, S.C. (2006) 'Properties of alumina particulate reinforced aluminum alloy produced by pressure die casting', *Materials and Design*, Vol. 27, No. 8, pp.676–683.

Shorowordi, K.M., Laoui, T., Haseeb, A.A., Celis, J.P. and Froyen, L. (2003) 'Microstructure and interface characteristics of B4C, SiC and Al_2O_3 reinforced al matrix composites: a comparative study', *Journal of Materials Processing Technology*, Vol. 142, No. 3, pp.738–743.

Singh, K., Rajput, S.K. and Mehta, Y. (2016) 'Modeling of the hot deformation behavior of a high phosphorus steel using artificial neural networks', *Materials Discovery*, Vol. 6, pp.1–8.

Sundaram, N.S. and Murugan, N. (2010) 'Tensile behavior of dissimilar friction stir welded joints of aluminium alloys', *Materials and Design*, Vol. 31, No. 9, pp.4184–4193.

Tian, D. and Shi, Z. (2018) 'MPSO: modified particle swarm optimization and its applications', *Swarm and Evolutionary Computation*, Vol. 41, pp.49–68.

Yang, X.S. and He, X. (2013) 'Firefly algorithm: recent advances and applications', *International Journal of Swarm Intelligence*, Vol. 1, No. 1, pp.36–50.

Zervoudakis, K. and Tsafarakis, S. (2020) 'A mayfly optimization algorithm', *Computers and Industrial Engineering*, Vol. 145, p.106559.

Zurada, J.M. (1992) *Introduction to Artificial Neural Systems* (Vol. 8), St. Paul, West.